

# Adsorbate induced manipulation of 1D atomic nanowires: Soliton mediated degradation of long-range order in the Si(553)-Au system

B. Hafke,\* T. Witte, and M. Horn-von Hoegen  
*Department of Physics and Center for Nanointegration (CENIDE),  
University of Duisburg-Essen, 47057 Duisburg, Germany*  
(Dated: November 27, 2019)

Deposition of Au on vicinal Si(553) surfaces results in the self-assembly of one-dimensional (1D) Au atomic wires. Charge transfer from the Au wire to the Si step edge leads to a chain of Si dangling-bond orbitals with a long range ordered threefold periodicity along the steps and finite interchain interaction perpendicular to the steps. Employing spot-profile analysis low-energy electron diffraction (SPA-LEED) we observed a broadening of spot width with time, reflecting the degradation of Si dangling bond chain and Au wire length. Adsorbates were identified as primary source for spot broadening. They force the generation of solitons and anti-solitons which immediately destroy the long-range order along and perpendicular to the steps, respectively. From the temporal evolution of broadening, we conclude that the Au wires are less reactive to adsorption than the Si dangling bond chains.

## Introduction and motivation

The assembly of single atoms to wires has recently attracted much attention, because such one-dimensional (1D) structures exhibit unique physical properties [1, 2]. The intrinsic low dimensionality of such systems causes pronounced instabilities in the electronic and structural degrees of freedom resulting in cooperative phenomena like the formation of charge density waves or spin density waves, depending on the interaction strength between electron system and lattice [3, 4]. Additionally, the interactions within the surface layer is crucial in the long-range ordering of the wires. Highly ordered arrays of atomic wires can be fabricated by self-assembly through the deposition of metal atoms on well defined vicinal semiconductor surfaces [5, 6]. Varying the substrate's vicinality allows the manipulation of interwire coupling and results in the modification of physical properties like the surface conductance [7, 8]. The understanding of such fundamental interaction mechanisms may lead to the utilization of 1D metallic wires as a toolbox for the fabrication of 2D and 1D systems with individually tailored properties [6]. However, for these applications the fragility of such systems is crucial, but has not been studied to far and thus warrants further investigation.

In this context, Au nanowires on the Si(553) surface have attracted a lot of attention. The formation of Au double-strands with dimerization along the steps is observed [9, 10]. Adjacent wires do not show a long-range correlation across the steps, but only minor electronic interactions with the Si atoms [11, 12]. The step edge is formed by a Si honeycomb-like structure. Due to charge redistribution within the surface layer every third Si step-edge atom along the steps exhibits an unsaturated dangling-bond (DB) orbital. It has been reported that this DB has a single electron occupation which leads to the intrinsic full spin polarization of this DB state [6, 13]. The condensation of these spins into an (anti-

)ferromagnetic DB array could be ruled out through the observation of ordering of DBs perpendicular to the steps: A centered-like geometry of the Si DB unit cell results in a magnetically frustrated array that favors a 2D quantum spin liquid phase rather than (anti-)ferromagnetic ordering [14].

The latest modification of the structural model predicts every third Si DB orbital to be unoccupied, which leads to the complete extinction of spin-interaction between the adjacent Si DB chains [12]. The much stronger interstep interaction between the Si DB chains compared to the Au wires can be attributed to Coulomb interactions of the partially charged DBs.

Here we report, that ordering of the DB chains and Au wires in 1D and 2D is fragile and readily affected by adsorbates. In a microscopic picture, solitons induce translational phase shifts in the Si DB chain and Au wire structure, respectively, resulting in gradual loss of long range order. Employing spot-profile analysis low-energy electron diffraction (SPA-LEED) [15, 16], we quantitatively describe the reduction of Si chain and Au wire lengths along the steps and the loss of long-range order perpendicular to the steps.

## Methods and sample system

The experiments were performed under ultra-high vacuum conditions (UHV) at a base pressure below  $1 \cdot 10^{-10}$  mbar. The substrate was cut from a *n*-type Si(553) wafer (phosphorus doped,  $0.01 \Omega\text{cm}$ ) with a nominal mis-cut of  $< 0.5^\circ$  and mounted on a liquid helium cryostat. Prior to deposition the sample was degassed at  $650^\circ\text{C}$  for several hours. The sample was cleaned in several short flash-anneal cycles by heating via direct current to  $1250^\circ\text{C}$ . An amount of 0.48 ML (monolayer, referred to the atomic density of a Si(111) surface, i.e.,  $1 \text{ ML} = 7.83 \cdot 10^{14} \text{ atoms/cm}^2$ ) Au was deposited from

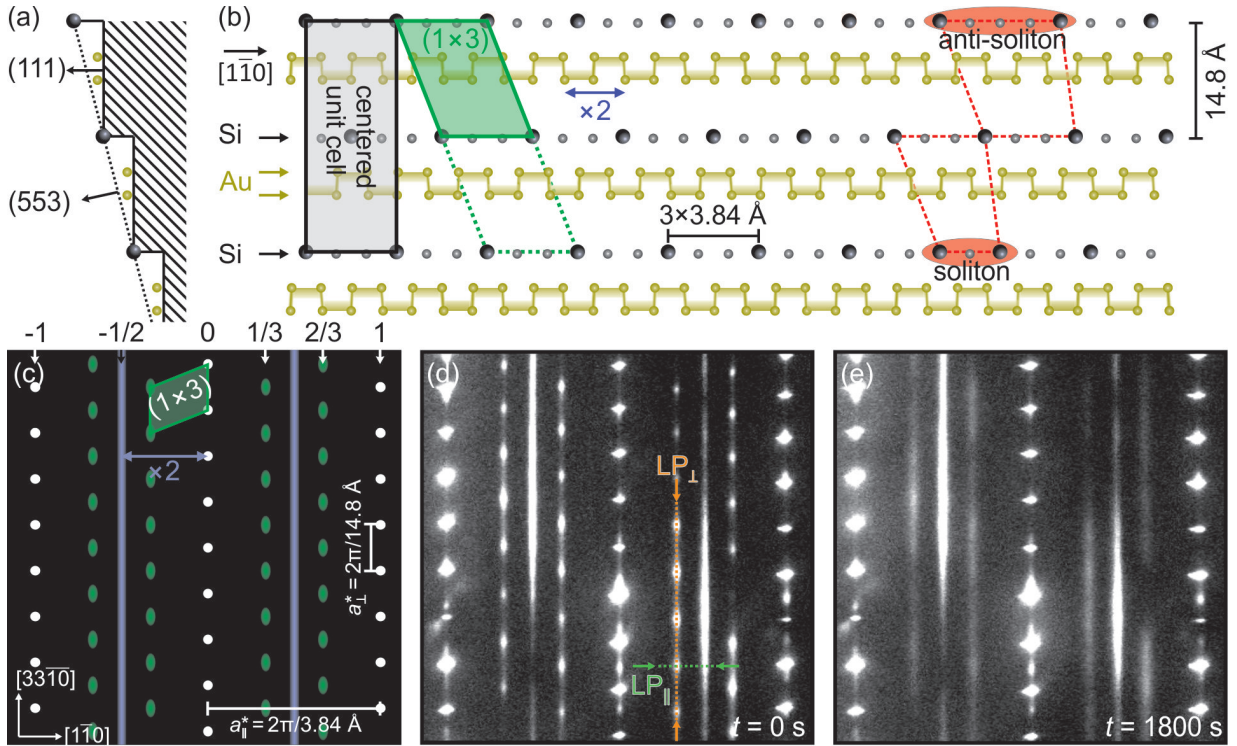


Figure 1. (a,b) Schematic structure model of the Si(553)-Au surface. Side view in (a) reveals terraces with (111) orientation. Top view of (b) shows the dimerized Au atoms as golden spheres, the saturated Si DBs as small gray spheres, and the unsaturated Si DBs as large gray spheres. The geometry of the Si DB array can either be described by the primitive  $(1 \times 3)$ -unit cell in green or by the centered unit cell in gray. In the right part a soliton and an anti-soliton is indicated as red ellipse, respectively. (c) Schematic LEED pattern of the perfect structure. The rows of integer order spots are indicated as white circles, the  $\times 3$  spots as green ellipses, and the  $\times 2$  streaks in blue lines. (d) LEED pattern at  $t = 0$  s directly after preparation shows perfect agreement with the ideal pattern from (c). (e) LEED pattern at  $t = 1800$  s after preparation shows clear broadening of the  $\times 3$  spots. All patterns were recorded at  $E = 150$  eV and a temperature of  $T = 78$  K.

an electron beam heated graphite crucible [17] at a substrate temperature of  $650^\circ\text{C}$ . The deposition was fol-

Figure 1 (a,b) show a schematic structure model of the Si(553)-Au system. Each step has a height of  $3.14 \text{ \AA}$  and is separated by terraces of  $14.4 \text{ \AA}$  width with a (111) orientation, as indicated in the side view of Fig. 1 (a). Accordingly, the Si(553) surface exhibits a miscut of about  $12.3^\circ$  with respect to the (111) orientation. The steps in the  $[3\bar{3}\bar{1}0]$  direction are separated by  $a_\perp = 14.8 \text{ \AA}$ , as sketched in the top view of Fig. 1 (b). The atomic distance along the step direction of the commensurate structure is  $a_0 = 3.84 \text{ \AA}$ . The Au double-strand wires (golden spheres) decorate the middle of the steps along the  $[1\bar{1}0]$  direction. The dimerization of the Au wires is indicated by alternating long and short interatomic distances, respectively. The Si step edge atoms are sketched as gray spheres. Every third Si atom along the steps (larger gray spheres) is embedded into a 2D array of unsaturated DBs forming a centered-like unit cell (gray shaded rectangle).

A schematic diffraction pattern resulting from this surface is shown in Fig. 1 (c). Three dense rows of integer order spots (white dots and indicated by -1, 0 and

lowed by a post annealing step [18] at  $850^\circ\text{C}$  for several seconds and subsequent rapid cooling to a temperature of  $T = 60$  K or  $T = 80$  K, respectively.

1) reflect diffraction from the periodic step train of the Si(553) substrate. The narrow distance of  $2\pi/14.8 \text{ \AA}$  between the integer order spots along the  $[3\bar{3}\bar{1}0]$  direction is caused by the step separation  $a_\perp$ . The wide separation of  $2\pi/3.84 \text{ \AA}$  reflects the spacing  $a_0$  of the Si atoms along the step. Two additional periodicities along the  $[1\bar{1}0]$  direction, i.e., between the rows of integer order spots can be identified. First, the streaks (light blue line) located half between the rows of integer order spots are caused by the twofold ( $\times 2$ ) periodicity of the dimerized Au wires. The dimerization between Au wires of adjacent terraces is almost uncorrelated and thus a streak instead of spots appears. Second, rows of weaker spots with a separation of  $2\pi/14.8 \text{ \AA}$  (elongated green dots) arise at positions  $1/3$  and  $2/3$  between the rows of integer order spots. These superstructure spots reflect the threefold ( $\times 3$ ) periodicity of the DB chain along the Si step edge. The primitive  $(1 \times 3)$ -unit cell and the centered unit cell are depicted in green and gray, respectively.

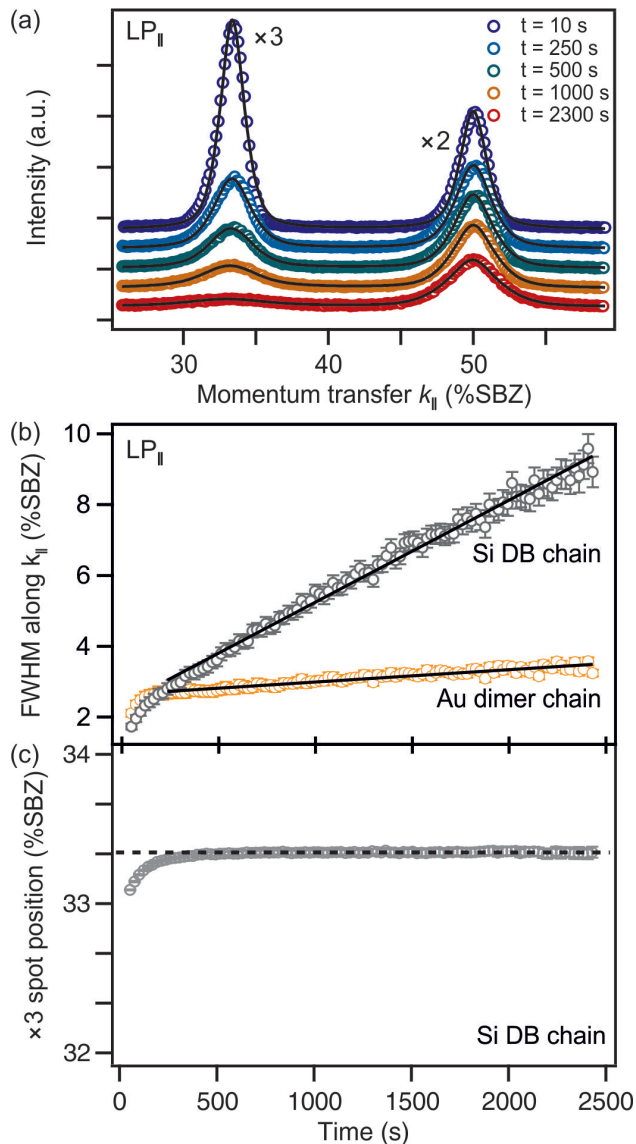


Figure 2. (a) Time series of spot profiles recorded at  $T = 60$  K perpendicular to  $\times 3$  spots and  $\times 2$  streaks (LP indicated as green dotted line in Fig. 1 (d)) indicating the evolution of long-range order along the Si DB chains and Au wires with time, respectively. LPs are shifted vertically for clarity. (b) The FWHM ( $100 \text{ \%SBZ} = 2\pi/3.84 \text{ \AA}$ ) of  $\times 3$  spots (from the Si DB chains) and  $\times 2$  streaks (from the Au wires) as determined from Lorentzian fits to the LPs shown in (a) in dependence of adsorption time. Black solid lines indicate linear FWHM increase with time. (c) The Position of the  $\times 3$  spot is independent on adsorption time for  $t > 200$  s (black dashed constant line).

## Results

After preparation of the Si(553)-Au surface and rapid cool down to 80 K we observe a continuous degradation of the initial LEED pattern with time. Figure 1 (d, e) depict the LEED patterns as prepared ( $t = 0$  s) and after

$t = 1800$  s of adsorption, respectively. The patterns are shown in a linear intensity scale to emphasize the relevant features of the superstructure spots and thus the integer order spots are overexposed. While the LEED pattern in Fig. 1 (d) at  $t = 0$  s exhibits clear spots at  $1/3$  position, these spots are strongly broadened in Fig. 1 (e) at  $t = 1800$  s both in the  $[1\bar{1}0]$  and in the  $[3\bar{3}\bar{1}0]$  direction.

Short flash-anneal cycles of few seconds duration up to  $850^\circ\text{C}$  result in desorption of adsorbates, no depletion or loss of Au coverage occurs [19], and the surface structure can be refreshed. The LEED pattern exhibits sharp spots again, i.e., the initial surface preparation is completely restored. As we do not observe any degradation of the LEED pattern through electron irradiation, we have to conclude evidence for adsorbate (from residual gas) induced broadening of the superstructure  $\times 3$  spots and  $\times 2$  streaks.

In order to quantify the increase of spot broadening we recorded - as function of adsorption time - intensity line profiles perpendicular and parallel to the streaks in the diffraction pattern, i.e., the  $[1\bar{1}0]$  direction (indicated through  $LP_{\parallel}$  in Fig. 1 (d) by the dotted green line), and perpendicular to the DB chains, i.e., the  $[3\bar{3}\bar{1}0]$  direction (indicated by  $LP_{\perp}$  in Fig. 1 (d) by the dotted orange line), respectively. All LPs are recorded at a base temperature of  $T = 60$  K. Fig. 2 (a) depicts selected line profiles along  $LP_{\parallel}$  as function of adsorption time. These line profiles through the  $\times 3$  spot and  $\times 2$  streak reflect the order along the Si DB chains and along the dimerized double-strand Au wires, respectively.

The profiles for the  $\times 3$  spot and  $\times 2$  streak are both described by Lorentzian functions

$$\mathcal{L}(k, \kappa) \propto \frac{1}{\kappa^2 + (k - k_0)^2} \quad (1)$$

with peak position  $k_0$  and full width at half maxima (FWHM) of the surface Brillouin-zone (SBZ),  $\text{FWHM} = 2\kappa$ , without any traces of a sharp central spike (see the solid lines in Fig. 2 (a)). The evolution of the related full width at half maxima (FWHM) for the  $\times 3$  spot and  $\times 2$  streak in dependence of adsorption time is shown in Fig. 2 (b). The curves exhibit a linear increase of FWHM with time of  $(0.173 \pm 0.002) \text{ \%SBZ/min}$  and  $(0.021 \pm 0.001) \text{ \%SBZ/min}$  for the  $\times 3$  spot and  $\times 2$  streak, respectively. For the very initial regime of adsorption the slope is even steeper and may be attributed to a crossover from 2D order to 1D order [20]. The position of the  $\times 3$  spot is plotted in Fig. 2 (c). Except for a small deviation at the initial regime of adsorption the position stays constant at  $1/3$  of the distance between the rows of integer order spots.

Fig. 3 (a) depicts selected spot profiles  $LP_{\perp}$  along the row of  $\times 3$  spots in  $[3\bar{3}\bar{1}0]$  direction (reflecting the real space order between adjacent Si DB chains) as function of adsorption time. These profiles are described by a sum of equidistant Lorentzian functions with identical FWHM

and without any traces of central spikes. With increasing adsorption time the spots rapidly broaden until at  $t = 1000$  s only a streak at  $1/3$  position between the row of integer order spots remains (see diffraction pattern in Fig. 1 (e)). The evolution of the corresponding FWHM in  $[3\bar{3}1\bar{0}]$  direction for the row of  $\times 3$  spots in dependence of adsorption time is shown in Fig. 3 (b). The curve exhibit an initial increase of FWHM with time of  $(2.70 \pm 0.08)$  %SBZ/min. Thus, the spot broadening of the  $LP_{\perp}$  direction increases faster with exposure time to residual gas than for the  $LP_{\parallel}$  direction.

### Discussion

In diffraction spot profiles with Lorentzian shape are indicative for the presence of anti-phase translational domains which exhibit a geometric size distribution [21–24]. The lateral and/or vertical phase shift may thereby arise from steps associated with islands on flat surfaces [22, 23], steps at vicinal surfaces ([24–26], or domain boundaries of superstructure domains [27, 28].

First, the mechanism for adsorbate induced spot broadening on the basis of the  $\times 3$  spots arising from the Si DB chains at the step edges is discussed. As we do not observe a systematic variation of the spot profiles with the vertical momentum transfer, we can exclude morphological changes of the surface during adsorption. Instead, we interpret the Lorentzian spot profile as a signature of ordered Si DB chains with  $\times 3$  periodicity with finite lengths (1D domains). Then, the length distribution of such 1D domains of ordered DB chains is a geometric distribution that is indicative for a Markov process [29]. Our experiment is sensitive to a maximum length limited by the instrumental transfer width of  $\xi \approx 30$  nm. The chains are confined by adsorbates originating from the residual gas. These adsorbates stick at the highly reactive Si step edges [8] and pinpoint the positions of the  $\times 3$  ordering of the Si DB chain with respect to the neighboring chains. Inevitably, this leads to the generation of heavy or light zero dimensional anti-phase domain boundaries, i.e., of solitons or anti-solitons, respectively [20]. Both types of solitons are schematically visualized in the right part of Fig. 1 (b) highlighted through red ellipses. The solitons and anti-solitons result in a shift of the  $\times 3$  Si DB by  $\pm a_0$  along the steps. As the position of the  $\times 3$  spots does not change during adsorption we conclude, that both, solitons and anti-solitons are generated with the same probability independent on the density of adsorbates.

The absence of a sharp central spike in the spot profiles indicates the loss of the long-range  $\times 3$  order in the Si DB chains already with the adsorption of the very first adsorbates. Thus, the entire Si DB chain is shifted along the steps and is only confined by other pinning defects or solitons. Solitons are mobile at finite temperatures

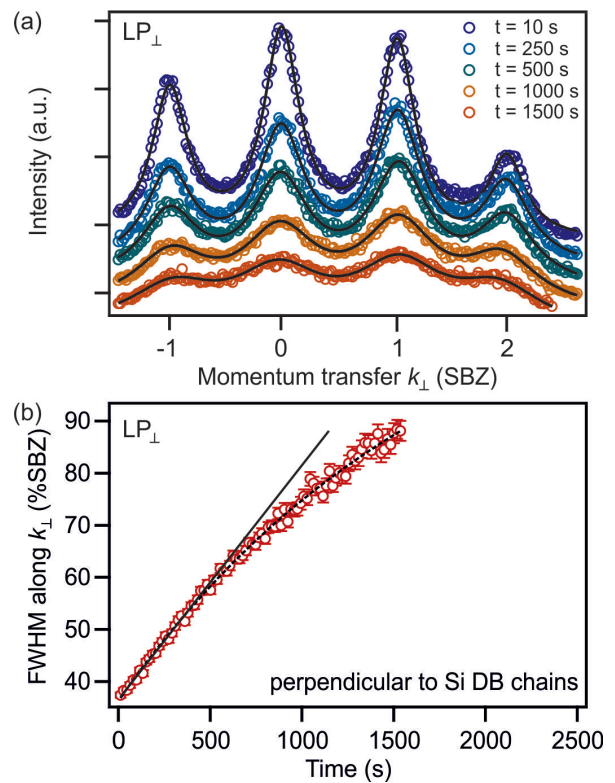


Figure 3. (a) Series of line profiles recorded at  $T = 60$  K along the row of  $\times 3$  spots ( $LP$  indicated as orange dotted line in Fig. 1 (d)) indicating the evolution of long-range order of Si DB chains perpendicular to the steps with time.  $LP$ s are shifted vertically for clarity. (b) The FWHM ( $100 \text{ \%SBZ} = 2\pi/14.8 \text{ \AA}$ ) as determined from a series of equidistant Lorentzian functions fitted to the line profiles (indicated as black curves) shown in (a). The solid black line reflects the linear increase of FWHM in the beginning of adsorption. The dashed curve provides a guide to the eye.

[20, 30]. As the motion of a DB by  $\pm a_0$  is initiated by electron hopping without the necessity of bond breaking only a small energy barrier has to be overcome. This motion is accompanied by a relaxation of the related Si atomic positions [12, 13]. Thus, we expect this process to be much faster than the time between two independent adsorption events.

Vertical to the chains, the FWHM increases faster than along the chains. Thus, the long-range centered order between the DB chains of neighboring steps is destroyed faster. The adsorbate-induced generation of solitons or anti-solitons in each DB chain leads not only to phase shifts within the DB chain, but also to extended phase shifts between adjacent DB chains along the chain direction. The shift of the DBs by one single adsorbate already destroys the centered correlation to both neighboring chains and is therefore particularly destructive. With increasing adsorbate density and thus arbitrary sequence of  $\times 3$  ordered DB chains, the phase correlation between neighboring chains is lifted extremely efficiently.

Finally, the transition to streaks in diffraction (Fig. 3 (a) line profile at  $t = 1500$  s) reflects the associated complete loss of correlation between adjacent DB chains.

The observations for the  $\times 2$  streak arising from the dimerization of the Au wire is interpreted in a similar way as we have done for the  $\times 3$  Si DB chains. Adsorbates from residual gas on the Au wires trigger a flip of dimerization along the terraces. This phase shift of dimerization of  $\Delta\phi = \pi$  is the fundamental excitation of these wires and requires to overcome an energy barrier. Compared with the Si DB chains, where both solitons and anti-solitons are equally present and the number of possible states is three, the Au wires exhibit only two states and just one type of phase boundary, i.e., solitons only. In contrast to the Si DB chain the associated phase shift requires bond breaking and reformation of Au-Au bonds between the dimerized Au atoms within the wire [12]. The local perturbation through an adsorbate is strong enough to provide the necessary energy. As in the case for the Si DB chains the  $\times 2$  streaks arising from the Au wires do not exhibit a sharp central spike. Instead, the continuous increase of FWHM of the Lorentzian shaped  $\times 2$  streak also indicates the immediate loss of long-range order of dimerized Au atoms.

Since the rise of FWHM (golden data points in Fig. 2 (b)) for the Au wires is less steep than for the DB chains, we conclude that the Au wire is less reactive to adsorption. This is also supported by DFT calculations [8] where the preferred adsorption sites for  $O_2$  are located at the Si step edge and not on the Au wires located in the middle of the terrace. From the vastly different slopes of the FWHM attributed to the Si DB chains and Au wires, we conclude that adsorbates on the Si DB chains have no influence to the long-range order of the Au wires, because otherwise the slope of change in FWHM would be the same for both adsorption sites.

### Summary and Conclusions

We studied adsorbate-induced degradation of long-range 1D and 2D ordered atomic wires in the Si(553)-Au system by means of SPA-LEED. A strong increase of spot width as function of adsorption time is indicative for a reduction of the lengths of  $\times 3$  ordered Si DB chains and  $\times 2$  dimerized Au wires length along the steps, respectively. This is explained by adsorbates forcing the generation of solitons or anti-solitons. From the absence of central spikes in the spot profiles we conclude that the long-range order of both Si DB chains and Au wires, respectively, is gradually degraded starting with the first adsorbates. The spot positions of the  $\times 3$  spots do not change with increasing adsorbate density proving that solitons and anti-solitons are generated with equal probability. We found a much lower reactivity of the Au wires compared to the Si DB chains. This corroborates the

findings of preferred adsorption sites to the Si step edge deduced from transport measurements and DFT [8]. The mechanisms of soliton/anti-soliton generation and soliton motion in the case of adsorption is closely related to thermal activation of soliton/anti-soliton pairs in that system [20]. Microscopically, the energies for these fundamental excitations which are mediated by the adsorbates have to be in the same order as the energies necessary for thermal excitations. We expect these processes which lead to the loss of long-range order also occur in other atomic wire systems of the Ge/Si( $h\bar{h}k$ )-Au family.

### Acknowledgments

Financial support via funding of the Deutsche Forschungsgemeinschaft (DFG, German Research Foundation) – Projektnummer 278162697 – SFB1242 project C03 "Driven phase transitions at surfaces: initial dynamics, hidden states and relaxation" is gratefully acknowledged. Financial support from the DFG FOR1700 research unit "metallic nanowires on the atomic scale: Electronic and vibrational coupling in real world systems" is gratefully acknowledged.

---

\* bernd.hafke@uni-due.de

- [1] H. W. Yeom, S. Takeda, E. Rotenberg, I. Matsuda, K. Horikoshi, J. Schaefer, C. M. Lee, S. D. Kevan, T. Ohta, T. Nagao, et al. Instability and charge density wave of metallic quantum chains on a silicon surface. *Phys. Rev. Lett.*, 82(24):4898, 1999.
- [2] F. J. Himpsel, K. N. Altmann, R. Bennewitz, J. N. Crain, A. Kirakosian, J. L. Lin, and J. L. McChesney. One-dimensional electronic states at surfaces. *J. Phys.: Condens. Matter*, 13(49):11097, 2001.
- [3] P. C. Snijders and H. H. Weitering. Colloquium: Electronic instabilities in self-assembled atom wires. *Rev. Mod. Phys.*, 82(1):307, 2010.
- [4] J. N. Crain, J. L. McChesney, Fan Zheng, M. C. Gallagher, P. C. Snijders, M. Bissen, C. Gundelach, S. C. Erwin, and F. J. Himpsel. Chains of gold atoms with tailored electronic states. *Physical Review B*, 69(12), mar 2004. doi:10.1103/physrevb.69.125401.
- [5] P. Segovia, D. Purdie, M. Hengsberger, and Y. Baer. Observation of spin and charge collective modes in one-dimensional metallic chains. *Nature*, 402(6761):504–507, December 1999. ISSN 0028-0836. URL <http://dx.doi.org/10.1038/990052>.
- [6] J. Aulbach, S. C. Erwin, R. Claessen, and J. Schäfer. Spin chains and electron transfer at stepped silicon surfaces. *Nano Letters*, 16(4):2698, 2016.
- [7] H. Okino, I. Matsuda, S. Yamazaki, R. Hobara, and S. Hasegawa. Transport in defective quasi-one-dimensional arrays of chains of gold atoms on a vicinal silicon surface. *Phys. Rev. B*, 76(3):035424, 2007.
- [8] F. Edler, I. Miccoli, J. P. Stöckmann, H. Pfnür, C. Braun, S. Neufeld, S. Sanna, W. G. Schmidt, and C. Tegenkamp.

- Tuning the conductivity along atomic chains by selective chemisorption. *Physical Review B*, 95(12), mar 2017. doi:10.1103/physrevb.95.125409.
- [9] W. Voegeli, T. Takayama, T. Shirasawa, M. Abe, K. Kubo, T. Takahashi, K. Akimoto, and H. Sugiyama. Structure of the quasi-one-dimensional si(553)-au surface: Gold dimer row and silicon honeycomb chain. *Phys. Rev. B*, 82:075426, Aug 2010. doi:10.1103/PhysRevB.82.075426. URL <http://link.aps.org/doi/10.1103/PhysRevB.82.075426>.
- [10] M. Krawiec. Structural model of the au-induced si(553) surface: Double au rows. *Phys. Rev. B*, 81:115436, Mar 2010. doi:10.1103/PhysRevB.81.115436. URL <http://link.aps.org/doi/10.1103/PhysRevB.81.115436>.
- [11] J. Aulbach, S. C. Erwin, J. Kemmer, M. Bode, J. Schäfer, and R. Claessen. Parity breaking in a double atomic chain system. *Phys. Rev. B*, 96:081406, Aug 2017. doi:10.1103/PhysRevB.96.081406. URL <https://link.aps.org/doi/10.1103/PhysRevB.96.081406>.
- [12] C. Braun, U. Gerstmann, and W. G. Schmidt. Spin pairing versus spin chains at si(553)-au surfaces. *Physical Review B*, 98(12), sep 2018. doi:10.1103/physrevb.98.121402.
- [13] S. C. Erwin and F. J. Himpsel. Intrinsic magnetism at silicon surfaces. *Nat. Commun.*, 1:58, 2010.
- [14] B. Hafke, T. Frigge, T. Witte, B. Krenzer, J. Aulbach, J. Schäfer, R. Claessen, S. C. Erwin, and M. Horn-von Hoegen. Two-dimensional interaction of spin chains in the si (553)-au nanowire system. *Physical Review B*, 94(16):161403, 2016.
- [15] U. Scheithauer, G. Meyer, and M. Henzler. A new leed instrument for quantitative spot profile analysis. *Surf. Sci.*, 178(1):441–451, 1986.
- [16] M. Horn-von Hoegen. Growth of semiconductor layers studied by spot profile analysing low energy electron diffraction-part i. *Z. f. Kristallographie*, 214(10):591–629, 1999.
- [17] P. Kury, R. Hild, D. Thien, H.-L. Günter, F.-J. Meyer zu Heringdorf, and M. Horn-von Hoegen. Compact and transferable threefold evaporator for molecular beam epitaxy in ultrahigh vacuum. *Rev. Sci. Instrum.*, 76(8):083906, 2005.
- [18] J. Aulbach, J. Schäfer, S. C. Erwin, S. Meyer, C. Loho, J. Settlein, and R. Claessen. Evidence for long-range spin order instead of a peierls transition in si(553)-au chains. *Phys. Rev. Lett.*, 111:137203, Sep 2013. doi:10.1103/PhysRevLett.111.137203. URL <http://link.aps.org/doi/10.1103/PhysRevLett.111.137203>.
- [19] M. Horn-von Hoegen, F.-J. Meyer zu Heringdorf, R. Hild, P. Zahl, T. Schmidt, and E. Bauer. Au-induced giant faceting of vicinal si (001). *Surface science*, 433:475–480, 1999.
- [20] B. Hafke, C. Brand, T. Witte, B. Sothmann, M. Horn-von Hoegen, and S. C. Erwin. Thermally-induced crossover from 2d to 1d behavior in an array of atomic wires: silicon dangling-bond solitons in si(553)-au. *submitted*, 2019.
- [21] M. Henzler. Quantitative evaluation of random distributed steps at interfaces and surfaces. *Surf. Sci.*, 73:240–251, 1978.
- [22] C. S. Lent and P. I. Cohen. Diffraction from stepped surfaces: I. reversible surfaces. *Surf. Sci.*, 139(1):121–154, 1984.
- [23] P. R. Pukite, C. S. Lent, and P. I. Cohen. Diffraction from stepped surfaces. *Surface Science*, 161(1):39–68, oct 1985. doi:10.1016/0039-6028(85)90727-7.
- [24] J. Wollschläger and C. Tegenkamp. Diffraction from disordered vicinal surfaces with alternating terraces. *Physical Review B*, 75(24), jun 2007. doi:10.1103/physrevb.75.245439.
- [25] S. Fölsch, G. Meyer, K.H. Rieder, M. Horn von Hoegen, T. Schmidt, and M. Henzler. Ag-mediated step-bunching instability on vicinal Si(100). *Surface Science*, 394(1-3):60–70, dec 1997. doi:10.1016/s0039-6028(97)00589-x.
- [26] C. Tegenkamp, J. Wollschläger, H. Pfnür, F.-J. Meyer zu Heringdorf, and M. Horn von Hoegen. Step and kink correlations on vicinal Ge(100) surfaces investigated by electron diffraction. *Physical Review B*, 65(23), may 2002. doi:10.1103/physrevb.65.235316.
- [27] T. Nagao, S. Hasegawa, K. Tsuchie, S. Ino, C. Voges, G. Klos, H. Pfnür, and M. Henzler. Structural phase transitions of si(111)-(3x3)r30-au: Phase transitions in domain-wall configurations. *Physical Review B*, 57(16):10100–10109, apr 1998. doi:10.1103/physrevb.57.10100.
- [28] R. Hild, F.-J. Meyer Zu Heringdorf, P. Zahl, and M. Horn-von Hoegen. Au induced regular ordered striped domain wall structure of a (5x3) reconstruction on si (001) studied by stm and spa-leed. *Surface science*, 454:851–855, 2000.
- [29] R. Spadacini and G. E. Tommei. A markovian approach to atomic scattering from rough surfaces. *Surface science*, 133(1):216–232, 1983.
- [30] S. C. Erwin and P. C. Snijders. Silicon spin chains at finite temperature: Dynamics of Si (553)-Au. *Physical Review B*, 87(23):235316, 2013.